PROCEEDINGS OF SCIENCE

# The Galactic population of Pulsar Wind Nebulae and the contribution of its unresolved component to the diffuse high energy gamma-ray emission

**Giulia Pagliaroli,**[a] **Saqib Hussain,**[b] **Vittoria Vecchiotti**[c] **and Francesco Lorenzo Villante**[a,d,*]

[a] *INFN-LNGS, I-67100 L'Aquila, Italy*
[b] *Gran Sasso Science Institute, 67100 L'Aquila, Italy*
[c] *NTNU, Department of Physics, NO-7491 Trondheim, Norway*
[d] *University of L'Aquila, Physics and Chemistry Department, 67100 L'Aquila, Italy*

*E-mail:* villante@lngs.infn.it

In the hypothesis that the majority of bright TeV sources detected by H.E.S.S. are powered by pulsar activity, like, e.g., pulsar wind nebulae (PWN) or TeV halos, we estimate the main properties of the Galactic pulsar population. We obtain a constraint on the spin-down time $\tau_{sd}$, the initial period $P_0$ and the magnetic field $B_0$. Evaluating the cumulative flux expected at Earth by the considered population, we show that unresolved PWNe contribute to the Galactic gamma-ray diffuse emission in the whole high-energy range from GeV to PeV. In particular, at TeV energy, their contribution could be as significant as 40% of the gamma emission due to resolved sources. We argue that unresolved PWNe could have also important implications for the interpretation of Fermi-LAT and Tibet AS$\gamma$ diffuse flux determinations in the GeV and sub-PeV energy domains.

38th International Cosmic Ray Conference (ICRC2023)
26 July - 3 August, 2023
Nagoya, Japan



*Speaker





PoS(ICRC2023)961

## 1. Introduction

The field of TeV $\gamma$-ray astronomy is rapidly evolving thanks to the data obtained by Imaging Atmospheric Cherenkov Telescopes (IACT), like H.E.S.S., MAGIC, VERITAS, and air shower arrays, such as Argo-YBJ, Milagro and HAWC. The TeV energy domain is particularly interesting for galactic studies. A guaranteed source of TeV radiation is the large scale diffuse emission produced by the interaction of cosmic-rays (CR) with $\sim$ PeV energies with the gas contained in the Galactic disk. In addition to diffuse emission, it also exists a comparable contribution from Galactic $\gamma-$ray sources that can emit radiation up to the PeV energy. The H.E.S.S. detector has presented a survey of 78 extended and point-like TeV $\gamma-$ray sources, the so-called H.E.S.S. Galactic Plane Survey (HGPS) [1] that includes a large part of the Galactic plane. Recently Tibet AS$\gamma$ [2] and HAWC [3] have shown that several Galactic sources produce $\gamma-$rays above $\sim$ 50 TeV. Moreover, LHAASO-KM2A reports the detection of more than 530 photons at energies above 100 TeV and up to 1.4 PeV from 12 ultra-high-energy $\gamma$-ray sources [4]. The emerging picture is that TeV Galactic sky is dominated by a population of bright sources powered by pulsar activity, such as Pulsar Wind Nebulae (PWNe) [1] or TeV halos [5–7].

In this review, following the lines of our previous works on this subject [8–11], we discuss the general properties of this source class. By assuming that TeV emission is proportional to the pulsar spin-down power, we model the luminosity function of galactic PWNe in terms of few parameters, namely the PWNe maximal luminosity $L_{\rm max}$ and fading (or spin-down) time scale $\tau_{\rm sd}$ (or, equivalently, the initial pulsar period $P_0$ and magnetic field $B_0$). These parameters can be constrained by using the HGPS observations [1], allowing us to estimate with relatively good accuracy the total luminosity and flux produced by galactic TeV PWNe. This also permits us to evaluate the cumulative emission from PWNe that cannot be resolved by H.E.S.S. This is particularly important because unresolved PWNe contribution could contaminate the large-scale diffuse signal observed at TeV by H.E.S.S. [12] and Milagro [13]. Moreover, since PWNe are expected to emit also at other energies (where, however, they can be less efficiently constrained, not being the dominant source class), their unresolved contribution can also have implications for the interpretation of Fermi-LAT and Tibet AS$\gamma$ diffuse flux determinations in the GeV and sub-PeV energy domains.

## 2. Method

We assume that spatial and intrinsic luminosity distribution of TeV PWNe can be written as:

$$\frac{dN}{d^3r\, dL} = \rho\left(\mathbf{r}\right) Y\left(L\right), \tag{1}$$

where $\mathbf{r}$ indicates the position in the Galaxy and $L$ is the $\gamma-$ray luminosity integrated in the energy range $1-100$ TeV probed by H.E.S.S.. The function $\rho(\mathbf{r})$, which is conventionally normalized to one when integrated in the entire Galaxy, is assumed to be proportional to the pulsar distribution in the Galactic plane parameterized by [14]. The source density along the direction perpendicular to the Galactic plane is assumed to scale as $\exp\left(-\left|z\right|/H\right)$ where $H = 0.2$ kpc represents the thickness of the Galactic disk.

If we assume that TeV-emission is powered by pulsar activity, it is reasonable to assume that TeV-luminosity is proportional to the pulsar spin-down power, i.e.:

$$L = \lambda \dot{E} \tag{2}$$

where $\lambda \leq 1$. The spin-down power decreases in time according to:

$$\dot{E} = \dot{E}_0 \left(1 + \frac{t}{\tau_{\rm sd}}\right)^{-2} \tag{3}$$

where:

$$\dot{E}_0 = \frac{8\pi^4 B_0^2 R_{\rm NS}^6}{3c^3 P_0^4} \qquad\qquad \tau_{\rm sd} = \frac{3Ic^3 P_0^2}{4\pi^2 B_0^2 R_{\rm NS}^6} \tag{4}$$

In the above relations, $P_0$ is the initial spin period and $B_0$ is the constant magnetic field, while the inertial momentum is $I = 1.4 \cdot 10^{45}\,{\rm g\,cm^2}$ and the pulsar radius $R_{\rm NS} = 12\,{\rm km}$ [15]. The parameter $\lambda$ in Eq.(2) is highly uncertain; it is determined by the conversion of the spin-down energy into $e^{\pm}$ pairs and by the subsequent production of TeV photons. It can be observationally determined for firmly identified PWNe in the HPGS catalog, obtaining values between $5 \times 10^{-5}$ and $6 \times 10^{-2}$, see Tab. 1 of [1]. For comparison, the value $\lambda \sim 3 \times 10^{-3}$ is provided in [6] by studying the TeV $\gamma-$ray emission of Geminga. In our approach, we consider $\lambda$ as a free parameter, taking the value $\lambda = 10^{-3}$ as a reference in numerical calculations. The possibility that $\lambda$ is correlated to the spin-down power, i.e.

$$\lambda = \lambda_0 (\dot{E}/\dot{E}_0)^{\delta} \tag{5}$$

has been recently suggested by the results of [1] that found $L = \lambda \dot{E} \propto \dot{E}^{1+\delta}$ with $1 + \delta = 0.59 \pm 0.21$ by studying a sample of PWNe in the HPGS catalog. By using Eqs.(2, 3, 5), we conclude that the source intrinsic luminosity decreases over the time scale $\tau_{\rm sd}$ according to:

$$L(t) = L_{\rm max} \left(1 + \frac{t}{\tau_{\rm sd}}\right)^{-\gamma}, \tag{6}$$

where $\gamma = 2\,(1 + \delta)$ and $L_{\rm max} = \lambda_0 \dot{E}_0$ is the initial luminosity. Assuming that the birth-rate $dN/dt = R$ of these sources in the Galaxy is constant in time, where $R = \varepsilon R_{\rm SN}$ with $\varepsilon \leq 1$ and $R_{\rm SN} = 0.019\,{\rm yr^{-1}}$ is the core-collapse Supernova rate recently measured by [16], we can calculate their luminosity distribution, $dN/dL = Y(L)$, that is given by:

$$Y(L) = \frac{R\,\tau_{\rm sd}\,(\alpha - 1)}{L_{\rm max}} \left(\frac{L}{L_{\rm max}}\right)^{-\alpha} \tag{7}$$

where $\alpha = 1/\gamma + 1$. In the above relation, the luminosity is allowed to vary in the range $L_{\rm min} \leq L \leq L_{\rm max}$ with the lower bound given by $L_{\rm min} \equiv L(T_{\rm d})$, where $T_{\rm d}$ is the total duration of the TeV-emission. The luminosity function in Eq. (7) is obtained by assuming, for simplicity, that all sources have approximately the same values for the initial period $P_0$ and magnetic field $B_0$ (and, consequently, the same maximal luminosity $L_{\rm max}$ and spin-down time $\tau_{\rm sd}$). We can, however, modify it to include the effects of dispersion of these parameters around reference values indicated as $\widetilde{P}_0$ and $\widetilde{B}_0$. In this case, we obtain:

$$Y(L) = \frac{R\,\widetilde{\tau}\,(\alpha - 1)}{\widetilde{L}} \left(\frac{L}{\widetilde{L}}\right)^{-\alpha} G\left(\frac{L}{\widetilde{L}}\right) \tag{8}$$

where $\widetilde{\tau} \equiv \tau_{\rm sd}(\widetilde{B}_0, \widetilde{P}_0)$ and $\widetilde{L} \equiv L_{\rm max}(\widetilde{B}_0, \widetilde{P}_0)$ are the spin-down time and maximal luminosity for the reference values $\widetilde{P}_0$ and $\widetilde{B}_0$. The obtained luminosity distribution differs from Eq. (7) for the presence of the function $G(L/\widetilde{L})$ that is given by:

$$G(x) \equiv \int dp\ h(p) p^{6-4\alpha} \int db\ g(b) b^{2\alpha-4}\, \theta\left(p^{-4}\, b^2 - x\right) \tag{9}$$

where $p \equiv P_0/\widetilde{P}_0$, $b \equiv B_0/\widetilde{B}_0$, while $h(p)$ and $g(b)$ describe the probability distributions of initial period and magnetic field. We assume that these functions can be modelled as gaussian distributions in $\log_{10}(p)$ and $\log_{10}(b)$, centered in zero and having widths given by $\sigma_{\log P} = \log_{10}(f_p)$ and $\sigma_{\log B} = \log_{10}(f_b)$ with the parameters $f_p$ and $f_b$ described in the next section. The important point to remark is that, when $f_p$ and $f_b$ are fixed, the luminosity distribution only depends on $\widetilde{\tau}$ and $\widetilde{L}$.

As it was shown in [8, 11], it is possible to constrain the source population by fitting the flux, latitude, and longitude distributions of bright sources in HGPS catalog. In order to avoid selection effects, we include in the fit only sources above the H.E.S.S. completeness threshold (i.e. having a flux above 1 TeV larger than 10% of that produced by CRAB, see [1]), excluding those firmly identified as Supernova Remnants. This corresponds to a sample of 29 sources that we consider to be pulsar-powered. This assumption is justified by the fact that 22 of these sources have a clear identification or a potential association with PWNe. The fit provides us an observational determination of the maximal luminosity $L_{\rm max}$ and of the spin-down time $\tau_{\rm sd}$. This permits to estimate the initial period $P_0$ and magnetic field $B_0$ of PWNe by using:

$$\begin{aligned} \frac{P_0}{1\,{\rm ms}} &= 94 \left(\frac{\lambda_0}{10^{-3}}\right)^{1/2} \left(\frac{\tau_{\rm sd}}{10^4 {\rm yr}}\right)^{-1/2} \left(\frac{L_{\rm max}}{10^{34}\,{\rm erg\,s^{-1}}}\right)^{-1/2} \\ \frac{B_0}{10^{12}{\rm G}} &= 5.2 \left(\frac{\lambda_0}{10^{-3}}\right)^{1/2} \left(\frac{\tau_{\rm sd}}{10^4 {\rm yr}}\right)^{-1} \left(\frac{L_{\rm max}}{10^{34}\,{\rm erg\,s^{-1}}}\right)^{-1/2} \end{aligned} \tag{10}$$

Moreover, the total Milky-Way luminosity in the 1-100 TeV energy range can be calculated as:

$$\mathcal{L}^{\rm MW} = \int dL\ Y(L)\, L = R \tau_{\rm sd}\, L_{\rm max}\, \frac{(\alpha-1)}{(2-\alpha)} \left[1 - \Delta^{\alpha-2}\right] \tag{11}$$

where $\Delta \equiv L_{\rm max}/L_{\rm min}$. The minimal luminosity $L_{\rm min}$ cannot be constrained by HESS observations and it is related to temporal duration of TeV PWNe emission, being $L_{\rm min} \equiv L_{\rm max}(1+T_{\rm d}/\tau_{\rm sd})^{-\gamma}$ with $\gamma = 1/(\alpha-1)$. However, its value marginally affects the quantities considered in this paper provided that $\Delta \gg 1$. The total flux produced by the considered population in the H.E.S.S. observational window (OW) is given by:

$$\Phi_{\rm tot} = \xi \frac{\mathcal{L}^{\rm MW}}{4\pi \langle E \rangle} \langle r^{-2} \rangle, \tag{12}$$

where $\langle E \rangle = 3.25$ TeV is the average energy of photons (see [8, 11] for details), $\xi \equiv \int_{\rm OW} d^3r\, \rho(\mathbf{r}) = 0.812$ represents the fraction of sources of the considered population which are included in the H.E.S.S. OW, while $\langle r^{-2} \rangle \equiv \frac{1}{\xi} \int_{\rm OW} d^3r\, \rho(\mathbf{r})\ r^{-2} = 0.0176\,{\rm kpc}^{-2}$ is the average value of their inverse square distance.

The above relationships are valid if $P_0$ and $B_0$ dispersions are neglected. If $P_0$ and $B_0$ dispersions are not negligible, one can still determine the average spin-down time $\widetilde{\tau}$ and maximal luminosity $\widetilde{L}$ of the PWNe population by fitting H.E.S.S. observational results. This allows us to

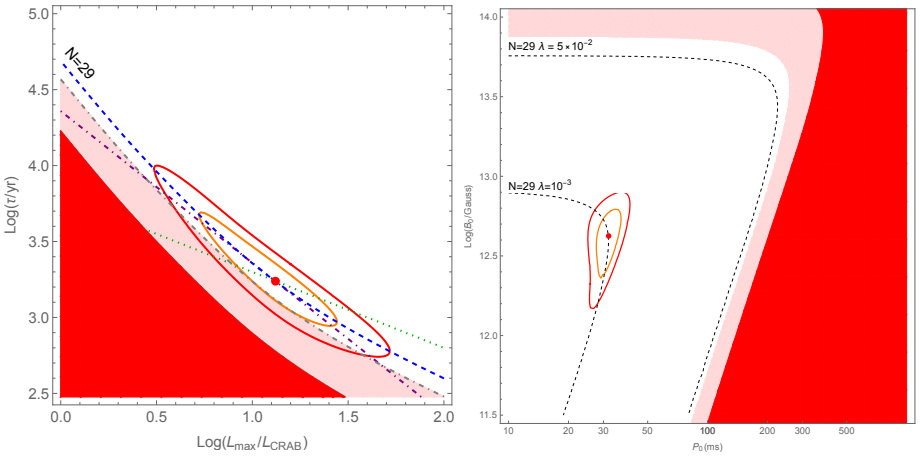


**Figure 1:** `Left Panel:` *The best fit and the* $1\sigma$ *and* $2\sigma$ *allowed regions in the plane* $(L_{\rm max}, \tau_{\rm sd})$. *The dark (light) red shaded area is excluded by the data because it corresponds to* $N(0.1\,\phi_{\rm CRAB}) \leq 10(22)$. `Right Panel:` *The best fit and the* $1\sigma$ *and* $2\sigma$ *allowed regions in the plane* $(P_0, B_0)$, *calculated in the assumption that* $\lambda = 10^{-3}$. *The dark (light) red shaded area is excluded because it corresponds to* $N(0.1\,\phi_{\rm CRAB}) \leq 10(22)$ *when we take* $\lambda = 5 \times 10^{-2}$ *as a realistic upper limit for the efficiency of TeV emission, see text for details.*

calculate the average initial period $\widetilde{P}_0$ and magnetic field $\widetilde{B}_0$ by using Eqs. (10) with the replacements $L_{\rm max} \to \widetilde{L}$ and $\tau_{\rm sd} \to \widetilde{\tau}$. The total source emission from the considered population is still calculated by using Eq.(12) with the total Milky-Way luminosity given by $\mathcal{L}^{\rm MW} = g\ (\alpha - 1)\ R\,\widetilde{\tau}\,\widetilde{L}$, where $g = \int dx\ G(x) x^{1-\alpha}$.

## 3. Results

Due to space limitations, we only discuss here our Reference case, obtained by assuming that the efficiency parameter $\lambda$ is constant[1]. In this case, the power-law index of the luminosity distribution is $\alpha = 1.5$. By maximizing the likelihood, we find the allowed regions displayed in the left panel of Fig. 1, corresponding to:

$$L_{\rm max} = 4.9^{+3.0}_{-2.1} \times 10^{35} {\rm erg\,s^{-1}} \qquad \tau_{\rm sd} = 1.8^{+1.5}_{-0.6} \times 10^3\ {\rm yr}, \tag{13}$$

The constraint on the maximal luminosity can be also expressed as $L_{\rm max} = 13^{+8}_{-6}\ L_{\rm CRAB}$ by considering that the CRAB luminosity (above 1 TeV) is $L_{\rm CRAB} = 3.8 \cdot 10^{34}\ {\rm erg\,s^{-1}}$. The above values can be used to determine through Eqs. (10) the initial period $P_0$ and magnetic field $B_0$ of the considered population. We get the constraints:

$$P_0 = 33.5^{+5.4}_{-4.3}\ {\rm ms} \times \left(\frac{\lambda}{10^{-3}}\right)^{1/2} \qquad B_0 = 4.3\,(1 \pm 0.45)\ 10^{12}\,{\rm G} \times \left(\frac{\lambda}{10^{-3}}\right)^{1/2} \tag{14}$$

that correspond to the regions in the right panel of Fig. 1. The small uncertainty for the period $P_0$ is connected with the fact that this quantity is determined by the product $L_{\rm max}\tau_{\rm sd}$ which is relatively well determined by observational data, being the possible variations of $L_{\rm max}$ and $\tau_{\rm sd}$ anti-correlated.

[1]The interested readers can find all the cases considered in our analisys in [8, 11] where the stability of our results with respect to adopted assumptions is also discussed.

The inferred magnetic field agrees with the value $\log_{10}(B_0/1G) \simeq 12.65$ obtained by pulsar population studies [17]. The best-fit period is consistent with the value $P_0 \sim 50\,\mathrm{ms}$ obtained in [18] by studying $\gamma-$ray pulsar population. On the other hand, the value $P_0 \sim 300\,\mathrm{ms}$ that is obtained from pulsar radio observation [17] seems excluded by our analysis, unless one assumes that a very large fraction $\lambda \sim 10^{-1}$ of the spin-down power is converted to TeV $\gamma-$ray emission.

The above results are obtained under the assumption that all the sources in the HGPS catalog with flux $\phi \geq 0.1\,\phi_{\mathrm{CRAB}}$ (except those firmly identified as SNRs) are powered by pulsar activity. A conservative upper bound for the period $P_0$ can be obtained by considering that no less than 10 of these sources have to be necessarily included in this population, being firmly identified as PWNe or Composite sources. The lines $N(0.1\,\phi_{\mathrm{CRAB}}) = \mathrm{const}$ corresponding to a fixed number of sources above the adopted flux threshold $0.1\,\phi_{\mathrm{CRAB}}$ are shown with gray dashed lines in the planes $(L_{\mathrm{max}},\,\tau_{\mathrm{sd}})$ and $(P_0,\,B_0)$ in Fig. 1. In particular, the dark red shaded area in Fig. 1 can be excluded because it corresponds to $N(0.1\,\phi_{\mathrm{CRAB}}) \leq 10$ and to the relatively large value $\lambda = 5 \times 10^{-2}$. If we consider that 12 additional sources in the HGPS catalog are considered as candidate PWNe on the basis of new data and/or phenomenological considerations [1, 3, 7, 19], the excluded region enlarges to the light red shaded area that corresponds to $N(0.1\,\phi_{\mathrm{CRAB}}) \leq 22$. This allows us to obtain the bound $P_0 \leq 260$ ms for $\alpha = 1.5$ and $\lambda = 5 \times 10^{-2}$ that can be strengthened if an upper limit for the magnetic field $B_0 \leq 10^{14}\,\mathrm{G}$ is introduced.

### 3.1 The TeV total and unresolved flux due to PWNe

By using Eqs. (11) and (12), we obtain a determination of the total luminosity of the Galaxy in the energy range $1 - 100\,\mathrm{TeV}$ and of the total flux (in the same energy range) produced by sources in the H.E.S.S. OW. We get:

$$\mathcal{L}_{\mathrm{MW}} = 1.7^{+0.5}_{-0.4} \times 10^{37}\,\mathrm{erg\,s^{-1}} \qquad \Phi_{\mathrm{tot}} = 3.8^{+1.0}_{-1.0} \times 10^{-10}\,\mathrm{cm^{-2}\,s^{-1}} \tag{15}$$

that correspond to $\mathcal{L}_{\mathrm{MW}} = 445^{+138}_{-112}\,L_{\mathrm{CRAB}}$ and $\Phi_{\mathrm{tot}} = 16.8^{+4.4}_{-3.5}\,\phi_{\mathrm{CRAB}}$ in CRAB units. The total TeV luminosity is only a factor $\sim 4$ smaller than that obtained in the energy range $1 - 100\,\mathrm{GeV}$ by fitting the Fermi-LAT 3FGL [20] and 1FHL [21] catalogs. These quantities are relatively well determined by observational data, due to the fact that they depend on the product $L_{\mathrm{max}}\,\tau_{\mathrm{sd}}$, see eqs. (11, 12).

The total flux $\Phi_{\mathrm{tot}}$ should be compared with the cumulative emission produced by all 78 resolved sources in the HGPS catalog, i.e. $\Phi_{\mathrm{HGPS}} = 10.4\,\phi_{\mathrm{CRAB}}$. The fact that $\Phi_{\mathrm{tot}}$ is substantially larger than $\Phi_{\mathrm{HGPS}}$ is not surprising. It is due to unresolved sources that are naturally expected to provide a relevant contribution to the total flux because the observational horizon for H.E.S.S. is limited, while sources are expected to be distributed everywhere in the Galaxy[2]. As it is discussed in [11], a lower (upper) bound for the unresolved flux is provided by the cumulative emission of faint sources with flux below H.E.S.S. sensitivity limit $0.01\,\phi_{\mathrm{CRAB}}$ (completeness threshold $0.1\,\phi_{\mathrm{CRAB}}$). By using this approach, we obtain $1.5\,\phi_{\mathrm{CRAB}} \leq \Phi_{\mathrm{NR}} \leq 5.4\,\phi_{\mathrm{CRAB}}$. A more refined estimate was obtained in [8] by subtraction, i.e. by calculating $\Phi_{\mathrm{NR}} = \Phi_{\mathrm{tot}} - \Phi_{\mathrm{HGPS}}$. Following [11], we consider here a conceptually equivalent approach but we include in the difference only sources with fluxes below $0.1\,\phi_{\mathrm{CRAB}}$, obtaining:

$$\Phi_{\mathrm{NR}} = \Phi_{\mathrm{F}}(0.1\,\phi_{\mathrm{CRAB}}) - \Phi_{\mathrm{F,\,HGPS}} = 3.9\,\phi_{\mathrm{CRAB}} \tag{16}$$

[2] As an example, a source with intrinsic luminosity $L \simeq L_{\mathrm{CRAB}}$ produces a flux larger than $0.1\,\Phi_{\mathrm{CRAB}}$, only at a distance smaller than $r \simeq 6$ kpc.

As it is discussed in [11], this value is more accurate because it is less sensitive to statistical fluctuations due to discrete distribution of sources in the Galaxy.

### 3.2 The relevance of unresolved PWNe for observations in the different energy domain

The estimated flux from unresolved PWNe is $\sim 40\%$ of the total resolved emission and it is likely to provide a relevant contribution to the diffuse large-scale $\gamma-$ray signal observed by H.E.S.S. and other experiments, with profound implications for the interpretation of observational results in the TeV domain. The unresolved flux $\Phi_{NR}$ is e.g. comparable to expectations for the truly diffuse contribution produced by the interaction of high-energy CR with the gas contained in the Galactic disk. Following the approach of [22] and [23], we estimated the diffuse component in the range $\Phi_{diff} = (5-15)\,\phi_{CRAB}$, depending on the assumed CR space and energy distribution. The estimate $\Phi_{diff} \simeq 15\,\phi_{CRAB}$ is obtained by assuming CR spectral hardening toward the Galactic center, as recently emerged from analysis of Fermi-LAT data at lower energies [24]. It was noted in [22] that, if unresolved contribution is large ($\Phi_{NR} \geq 0.5\,\Phi_{HPGS}$), this possibility is disfavoured by H.E.S.S. [12] because the total flux (resolved + unresolved + truly diffuse signal) obtained in this hypothesis exceeds the total observed emission from the Galactic plane. This conclusion was strengthened in [8] by noting that the total flux measured by Milagro at 15 TeV ($d\Phi/dE \sim 2.9\times10^{-12}\,cm^{-2}\,s^{-1}\,sr^{-1}\,TeV^{-1}$ for $30 < l < 65$ and $|b| < 2$) is consistent with the total flux produced by the HGPS source population in the same observation window ($d\Phi^{M}_{HGPS}/dE \sim 3.4\times10^{-12}\,cm^{-2}\,s^{-1}\,sr^{1}\,TeV^{-1}$). This suggests that the anomalous diffuse emission reported by Milagro is due to unresolved sources and provides an additional constraint to the possibility of a large truly-diffuse contribution produced by CR interactions in the Galactic disk.

Our results in the GeV and sub-PeV energy ranges discussed in [9] and [10] point in the same direction. In both cases, we need to extrapolate what we learned in the TeV range relying on suitable assumptions on the PWNe spectrum. In particular, the extension to the GeV energy range is delicate, and we use a phenomenological approach based on energy-integrated quantities of the identified PWNe observed in both GeV and TeV sources catalogs. The considered spectrum is consistent with theoretical predictions of PWNe emission and it can be refined in the future adopting a dynamical model for PWNe gamma-ray emission. Our analysis shows that the inferred cumulative contribution due to unresolved PWNe in the 1-100 GeV energy range is not negligible. The inclusion of this additional gamma-ray component in the analysis of the total diffuse emission measured by Fermi-LAT changes the inferred cosmic ray spectral index. Interestingly, when a fraction of the observed Fermi-LAT gamma-ray signal is associated to unresolved PWNe, the cosmic-ray spectral index moves in the direction to flatten its value to the local one as expected for standard assumption of cosmic-ray diffusion in the Galactic plane.

Moving to the sub-PeV energy range, we estimate the contribution due to unresolved PWNe in the two OWs of the Tibet AS$\gamma$ experiment. The prediction in this case only requires to introduce a spectral energy cutoff for the TeV PWNe population. Despite the value of the energy cutoff is uncertain, we show that unresolved PWNe provide a relevant contribution in this energy range unless the spectral energy cut-off moves below 100 TeV (in contrast with recent observations [25]). Moreover, the inclusion of unresolved PWNe contribution produces a better description of the Tibet AS$\gamma$ data than CR spectral hardening.

## References


[1] H. Abdalla et al. *Astron. Astrophys.*, 612:A2, 2018.

[2] M. Amenomori et al. *Phys. Rev. Lett.*, 126(14):141101, 2021.

[3] T. Sudoh, T. Linden, and D. Hooper. 1 2021.

[4] Z. Cao et al. *Nature*, 594(7861):33–36, 2021.

[5] T. Sudoh, T. Linden, and J. F. Beacom. *Phys. Rev. D*, 100(4):043016, 2019.

[6] T. Linden and B. J. Buckman. *Phys. Rev. Lett.*, 120(12):121101, 2018.

[7] G. Giacinti et al. *Astron. Astrophys.*, 636:A113, 2020.

[8] M. Cataldo, G. Pagliaroli, V. Vecchiotti, and F. L. Villante. *Astrophys. J.*, 904(2):85, 2020.

[9] V. Vecchiotti, G. Pagliaroli, and F. L. Villante. *Commun. Phys.* 5, 161, 2022.

[10] V. Vecchiotti, F. Zuccarini, F. L. Villante, and G. Pagliaroli. *Astrophys. J.*, 928(1):19, 2022.

[11] G. Pagliaroli, S. Hussain, V. Vecchiotti, and F. L. Villante, submitted to *Universe*, 2023.

[12] A. Abramowski et al. *Phys. Rev. D*, 90(12):122007, 2014.

[13] R. Atkins et al. *Phys. Rev. Lett.*, 95:251103, 2005.

[14] D. R. Lorimer et al. *Mon. Not. Roy. Astron. Soc.*, 372:777–800, 2006.

[15] J. M. Lattimer and M. Prakash. *Phys. Rept.*, 442:109–165, 2007.

[16] R. Diehl et al. *Nature*, 439:45–47, 2006.

[17] C.-A. Faucher-Giguere and V. M. Kaspi. *Astrophys. J.*, 643:332–355, 2006.

[18] K. P. Watters and R. W. Romani. *Astrophys. J.*, 727:123, 2011.

[19] S. P. Wakely and D. Horan. *International Cosmic Ray Conference*, 3:1341–1344, 2008.

[20] M. Ajello et al. *Astrophys. J. Suppl.*, 232(2):18, 2017.

[21] M. Ackermann et al. *Astrophys. J. Suppl.*, 209:34, 2013.

[22] M. Cataldo, G. Pagliaroli, V. Vecchiotti, and F. Villante. *JCAP*, 12:050, 2019.

[23] G. Pagliaroli, C. Evoli, and F. L. Villante. *JCAP*, 11:004, 2016.

[24] F. Acero et al. *Astrophys. J. Suppl.*, 223(2):26, 2016.

[25] A. Abeysekara et al. *Physical Review Letters*, 124(2), Jan 2020. ISSN 1079-7114.